

## C-axis Orientation and Growth Structure of AlN Thin Films on SiO<sub>2</sub>/Si Substrates Deposited by Reactive RF Magnetron Sputtering

Han-Yong Joo, Jae Bin Lee and Hyeong Joon Kim

School of Materials Science and Engineering, Seoul National University Seoul 151-742, Korea

(Received October 3, 1997)

Aluminum nitride (AlN) thin films were deposited on SiO<sub>2</sub>/Si substrates by reactive sputtering for the application of SAW devices. The major deposition parameters such as pressure, nitrogen fraction, rf power, substrate distance were changed to find out the optimal condition for c-axis oriented thin films on an amorphous substrate. The effects of deposition parameters on the crystal structure, residual stress, and growth morphology of thin films were characterized by XRD, SEM, and TEM. The FWHM of (002) rocking curve of the films deposited at the proper condition was lower than 2.2° ( $\sigma=0.93^\circ$ ). Cross-sectional TEM showed that self-aligned structure was developed just after slightly random growth at the initial stage. The frequency characteristics of test device fabricated from AlN thin films confirmed their piezoelectric property and applicability for SAW devices.

**key words** : AlN thin film, Sputtering, C-axis orientation, Residual stress, SAW.

### I. Introduction

There have been considerable efforts to use AlN (aluminum nitride) thin film as a material for high-frequency SAW (Surface Acoustic Wave) devices because of its high SAW velocity.<sup>1,8</sup> Since high degree of crystalline orientation and smooth interface and surface are necessary for its application of SAW devices, epitaxial thin films are most suitable, but epitaxy requires precise control of many factors such as purity of materials, selection of substrates, deposition temperature, background pressure, and cleanness of reactor system.<sup>9,10</sup>

Recently, Soh *et al.*<sup>7</sup> deposited AlN thin films on various substrates for the application of SAW devices and evaluated the crystalline orientation of these films by XRD rocking curves and pole figure patterns. The standard deviations in rocking curves of AlN thin films on SiO<sub>2</sub> (1000Å)/Si, Si<sub>3</sub>N<sub>4</sub> (2000Å), Si(100) and Si(111), are 2.6°, 3.1°, 2.6°, and 2.5°, respectively and pole figures also showed similar result. Both results mean that the crystallinity of a substrate does not affect a crystalline alignment of polycrystalline film, which is grown at rather loose condition than epitaxial condition. Akiyama *et al.*<sup>11</sup> deposited highly c-axis orientated AlN thin films on sintered MoSi<sub>2</sub> substrates and reported the effect of temperature on the structure and crystal orientation of the films.

In this study, we used silicon wafers with thermal oxide layer as substrates for AlN thin films, because SiO<sub>2</sub>/Si substrates are useful for hybrid devices or BAW (Bulk Acoustic Wave) devices.<sup>12-14</sup> AlN thin films were deposited by reactive rf magnetron sputtering system. The effects of deposition parameters on the growth structure and crystalline alignment of AlN thin films were in-

vestigated to solve the inherent problems of sputtered AlN thin films such as high residual stress and surface roughness. The applicability of AlN/SiO<sub>2</sub>/Si thin films for SAW devices was also examined.

### II. Experimental Procedure

The schematic diagram of rf magnetron sputtering system is shown in Fig. 1. Al metal target was located on one of three cathodes. Nitrogen gas was regulated by MFC (mass flow controller), and total pressure was regulated by pressure controller with a throttle valve in the Ar feed-line. Pumping rate was adjusted for suitable flow rate and pressure. The specifications of raw materials and deposition conditions are listed in Table 1. The 9.5 cm × 9.5 cm holder with 3.6 cm × 3.6 cm SiO<sub>2</sub>/Si substrate was clamped under circular plate in sputtering system. Presputtering was carried out for longer than 10 minutes with closed shutter in order to establish steady state of target surface and stable discharge condition.

The crystallinity and crystalline orientation of the films were determined by X-ray diffractometer (CuK $\alpha$  radiation, 35 kV, 20 mA). The degree of alignment was evaluated by measuring the FWHM (Full Width at Half Maximum) of rocking curves which were obtained from  $\omega$  scans. Growth morphology and film thickness were evaluated by SEM (scanning electron microscope). The fine growth-structure was observed by TEM (transmission electron microscope, Philips CM20).

The test SAW devices were fabricated to evaluate the SAW characteristics of AlN/SiO<sub>2</sub>/Si thin films. Frequency responses were measured by network analyzer (Advantest R3765C) under 50  $\Omega$  impedance, after a series of the

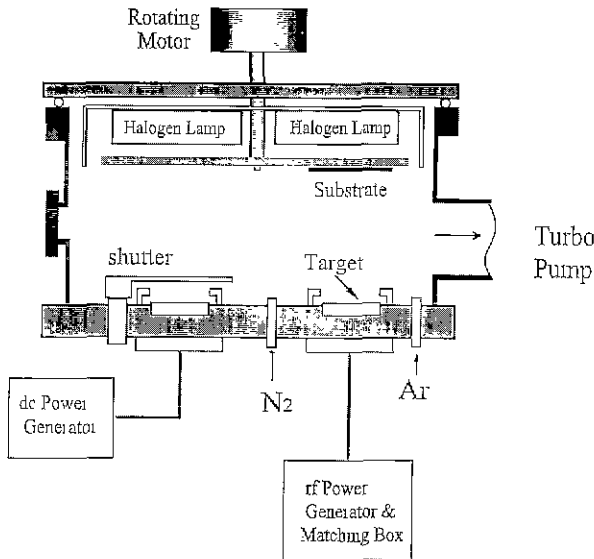


**Fig. 1.** Schematic Diagram of RF Sputtering System.

**Table 1.** Deposition Conditions

Equipment	RF magnetron sputtering system
Target	Al metal (5N), 3 inch dia.
Sputtering Gas	Ar(6N), N <sub>2</sub> (5N)
Background Pressure	$< 2 \times 10^{-5}$ Torr
Presputtering Time	10~20 min.
Sputtering Pressure	3~30 mTorr
Gas ratio (Ar/N <sub>2</sub> )	0~6
Substrates	SiO <sub>2</sub> /Si(100)
Substrate Temperature	self heating ~200 °C
RF power	90~210 W
Target substrate spacing	2~8 cm

fabrication processes consisting of Al deposition, IDT (interdigital transducer) electrode patterning, dicing, wire bonding and packaging.

### III. Results and Discussion

In the first step to figure out the optimal deposition condition, effects of sputtering pressure, target-to-substrate distance, rf power on the crystal structure of AlN thin films were investigated. Equal amount of Ar and N<sub>2</sub> gas, deposition time of 2 hrs, no intentional substrate heating (substrates were heated by plasma up to 100°C~150°C) were common conditions in these experiments. Fig. 2 shows some of the XRD patterns of thin films. The crystallinity and c-axis alignment were poor at the conditions of low pressure, high power, and short distance, while (002) preferred orientation appeared at high pressure (11 mTorr, Ar/N<sub>2</sub>=1) except at very short distance. These results show that precise pressure control and optimal substrate distance are essential for the deposition of AlN thin films with high degree of c-axis orientation. Another noticeable

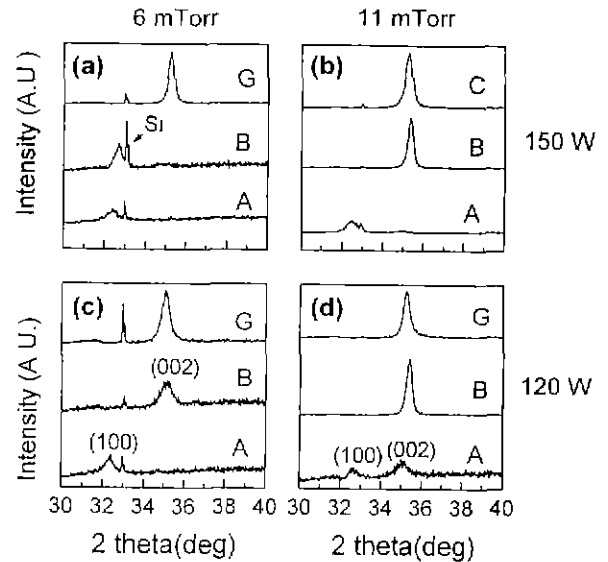


**Fig. 2.** XRD patterns of AlN thin films with various deposition conditions. (a) 6 mTorr and 150 W, (b) 11 mTorr and 150 W, (c) 6 mTorr and 120 W and (d) 11 mTorr and 120 W; A, B, C and G indicate substrate position, of which distance from target is 2 cm, 3 cm, 4 cm and 8 cm, respectively.

result is that lattice parameters of the films are 1.3% higher than that of standard sample (JCPDS 25-1133). The interplanar spacing of the films were in the range of  $d_{100}=2.73\text{--}2.76\text{\AA}$ , and  $d_{002}=2.53\text{--}2.55\text{\AA}$ , compared to  $d_{100}=2.695\text{\AA}$  and  $d_{002}=2.490\text{\AA}$  of AlN powder, indicating the presence of residual compressive stress in the films. Since the expansion of AlN film to in-plane direction is restricted by the adhesion with thick substrate, the film should expand to the growth direction. Thermal stress induced by different thermal contraction should be tensile, because thermal-expansion coefficient of AlN is larger than that of Si.<sup>5</sup> However, assuming elastic modulus,  $E_{\text{AlN}}=350\text{ GPa}$ ,<sup>16</sup> and Poisson ratio,  $\nu=0.3$ ,<sup>17</sup> 1.3% strain is equivalent to in-plane compressive stress of 6.5 GPa in a biaxial stress state. There have been many reports concerning the residual stress of AlN thin films.<sup>16-20</sup> Este *et al.*<sup>15</sup> observed that AlN thin films deposited by reactive sputtering in N<sub>2</sub> were und-

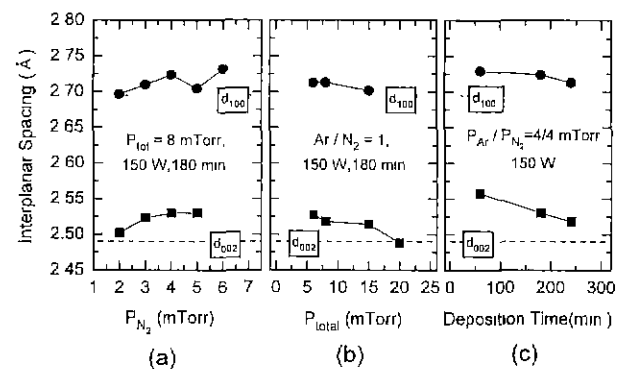


**Fig. 3.** Lattice parameter variation of AlN thin films: (a) with nitrogen pressure ( $P_{\text{N}_2}$ ), (b) with total pressure and (c) with deposition time.

er high compressive stress ( $\sim -3$  GPa) whereas stress-free films were obtained in 40% Ar atmosphere. Este and Westwood<sup>19)</sup> also showed that residual stress varied from -19 GPa (compressive) to +2.5 GPa as N<sub>2</sub> pressure was increased from 1.5 mTorr to 37.5 mTorr. The transition from compressive to tensile residual stress occurred at about 7.5 mTorr. They explained that high compressive stress was caused by atomic peening phenomena as a result of bombardment of energetic atoms reflected from target or sputtered negative ions which were accelerated away from the target. Small amount of oxygen impurity may cause the lattice strain and residual stress by incorporation into the lattice or bombarding effect.<sup>10)</sup>

The control of rf power is crucial for attaining high growth rate and dense structure from high surface mobility enhanced by bombardment. Fig. 4(a) shows that growth rate increases linearly with rf power. On the other hand, total pressure makes little difference in growth rate at the same nitrogen pressure except for 210 W condition. High energetic bombardment onto growing film would cause resputtering and nucleation of crystallites with different orientation in addition to mobility enhancement effect. Considering target voltage and scattering effect, resputtering becomes dominant at lower pressure, resulting in a suppression of growth rate at 210 W and Ar/N<sub>2</sub>=4/2 mTorr. It is generally recognized that growth rate is affected by geometry of system in addition to processing factors such as nitridation of target surface, scattering in the gas phase, and resputtering.<sup>19)</sup> Although higher growth rate than 200 Å/min. was achieved,<sup>21,22)</sup> the preferred orientation changed from (001) to (101) when the deposition rate exceeded 108 Å/min.<sup>23)</sup> Therefore it is hard to achieve high c-axis alignment and high growth rate simultaneously.

The AlN films deposited at 180 W appeared to have the most dense structure and good c-axis alignment regardless of total pressure. The degree of c-axis alignment in high-pressure condition (Ar/N<sub>2</sub>=6/2 mTorr) was generally better than that in low-pressure condition (Ar/N<sub>2</sub>=4/2 mTorr) as shown in Fig. 4(b).

Since residual stress and microstructure are sensitive

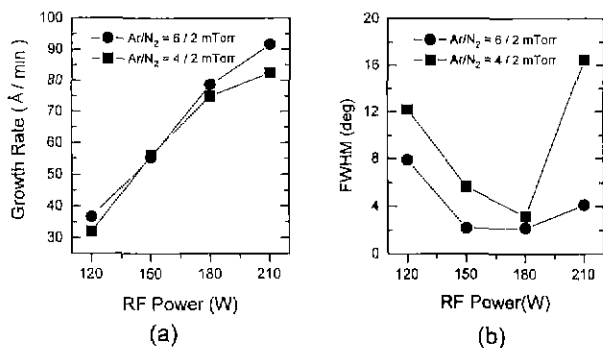


Fig. 4. Dependence of (a) growth rate and (b) FWHM (rocking curve) of AlN thin films on rf power.

to deposition pressure, total pressure was controlled by changing Ar flow at constant N<sub>2</sub> pressure (2 mTorr) and at constant rf power (180 W). As Ar pressure increased from 3 mTorr to 8 mTorr, degree of c-axis alignment showed maximum at 6 mTorr without a change of preferred orientation, and the (002) interplanar spacing decreased to 2.484 Å, which is lower than bulk value, as shown in XRD results of Fig. 5. The FWHM value of 2.17° (standard deviation  $\sigma=0.92^\circ$ ) is very good for a polycrystalline film, which is comparable to 1.33° of the epitaxial SiC thin film measured in the same condition.

Poor crystallinity and low growth rate under low pressure were probably due to lattice damage and resputtering effects induced by high energetic bombardment. The film deposited at low pressure (Ar/N<sub>2</sub>=3/2 mTorr) had wave-like surface morphology with poorly defined grain boundaries, as shown in Fig. 6. This sample had a mm-size flaws on the surface just after it was unloaded from the deposition chamber. After a few days, the peel-off process gradually progressed and finally it revealed the large area of fractured Si surface consisting of parallel wedges with small portion of the film. Although the origin of the flaws is uncertain yet, large residual stress probably caused the peel-off and resulted in the plucking-off of Si substrate owing to very strong adhesion at interface between film and SiO<sub>2</sub>/Si.

Surface and cross-sectional morphologies were changed as Ar pressure increased, as shown in Fig. 7. The film deposited at 4 mTorr contained a lot of 3 or 4 times larger grains compared to the normal grains, but that at 6 mTorr showed dense and smooth morphology having uniform grains of 500 Å diameter. The film deposited at higher Ar pressure of 8 mTorr had fibrous grains with loose boundaries. The good c-axis alignment was accompanied by dense and uniform microstructure. The film of 6 mTorr Ar and 2 mTorr N<sub>2</sub> had the best c-axis alignment

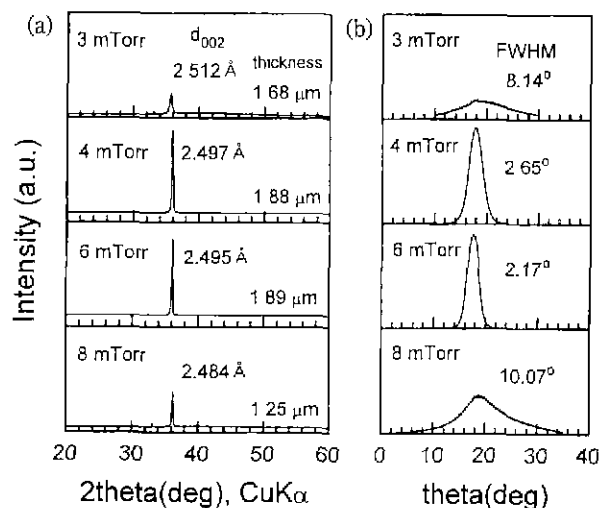
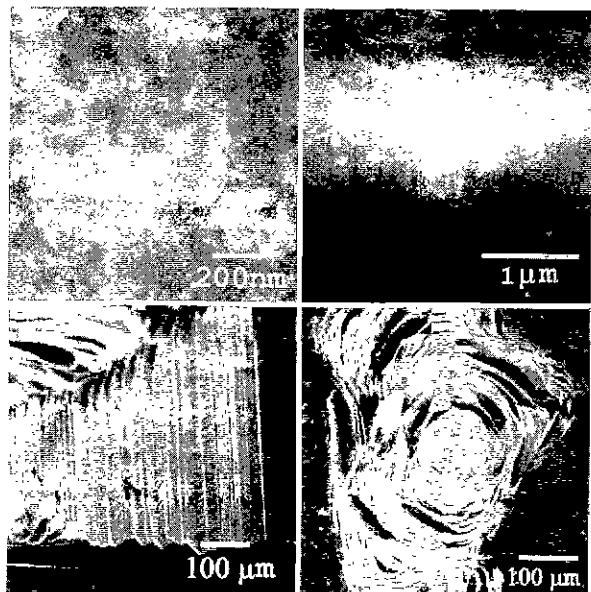


Fig. 5. XRD patterns of AlN thin films deposited at P<sub>N2</sub>=2 mTorr, 180 W and 200°C for 240 min., with various Ar pressures: (a) 2θ/θ scans and (b) rocking curves.

(FWHM=2.17°).

The change of growth morphology with Ar pressure can be explained with respect to kinetics of adatoms rather than thermodynamic aspect Thornton's 'micro-structure zone diagram' has been most popularly referred for explaining the growth morphologies of the films deposited by sputtering.<sup>23)</sup> But it was modified by Mes-

sier *et al.*<sup>20)</sup> to 'revised structure zone model' with adopting bombardment-induced mobility ( $V_b$ ) instead of Ar pressure, thermal-induced mobility ( $T/T_m$ ), and log scale thickness-axis to depict the evolutionary development of physical structure. According to these models, changing from dense zone-T (6 mTorr) to columnar zone-1 (8 mTorr) is attributed to the decrease of bombardment-induced energy related to the factors such as inelastic scattering in gas phase, incident angle broadening, and



**Fig. 6.** SEM micrographs of the AlN thin film deposited on SiO<sub>2</sub>/Si at Ar/N<sub>2</sub>=3/2 mTorr and 180 W, for 240 min.: the top left one is plan-view, the top right one is over-view and the others are the micrographs of typical plucked-off regions showing fractured surface.

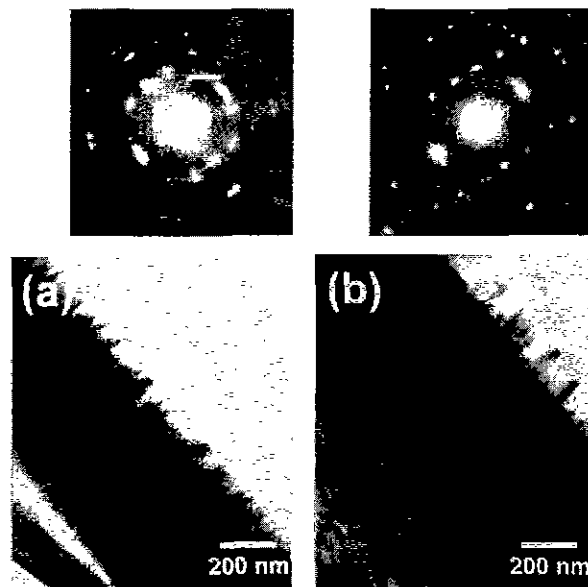


**Fig. 8.** TEM SADPs and bright field images of an AlN thin film deposited at Ar/N<sub>2</sub>=6/2 mTorr, 180 W: (a) near interface and (b) near surface.

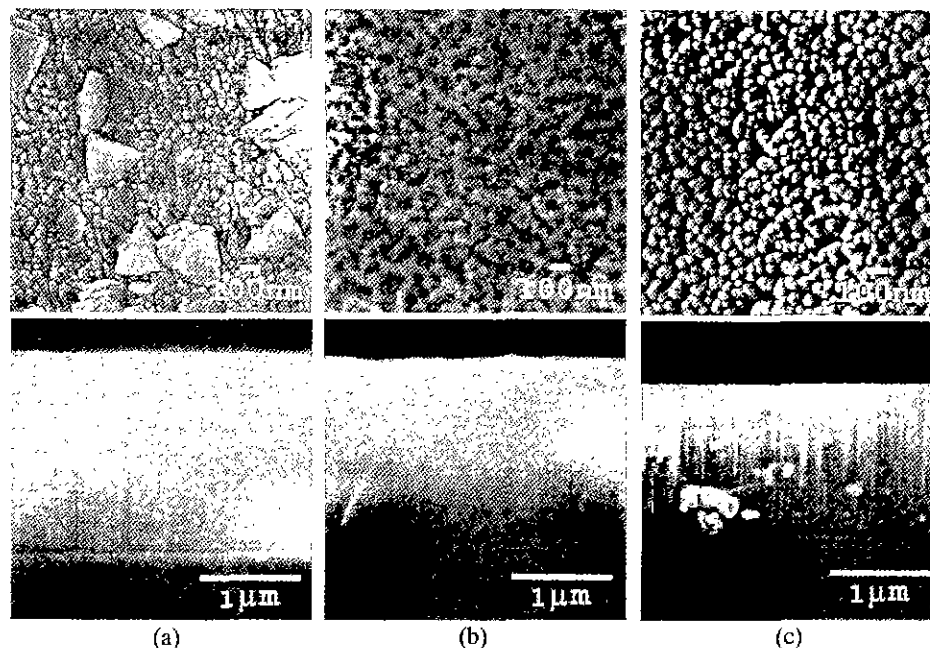


**Fig. 7.** SEM micrographs of AlN thin film deposited on SiO<sub>2</sub>/Si at 180 W for 240 min., with various Ar pressures: (a) 4 mTorr, (b) 6 mTorr and (c) 8 mTorr. The upper ones are the plan-view micrographs and the lower are the cross-sectional micrographs.

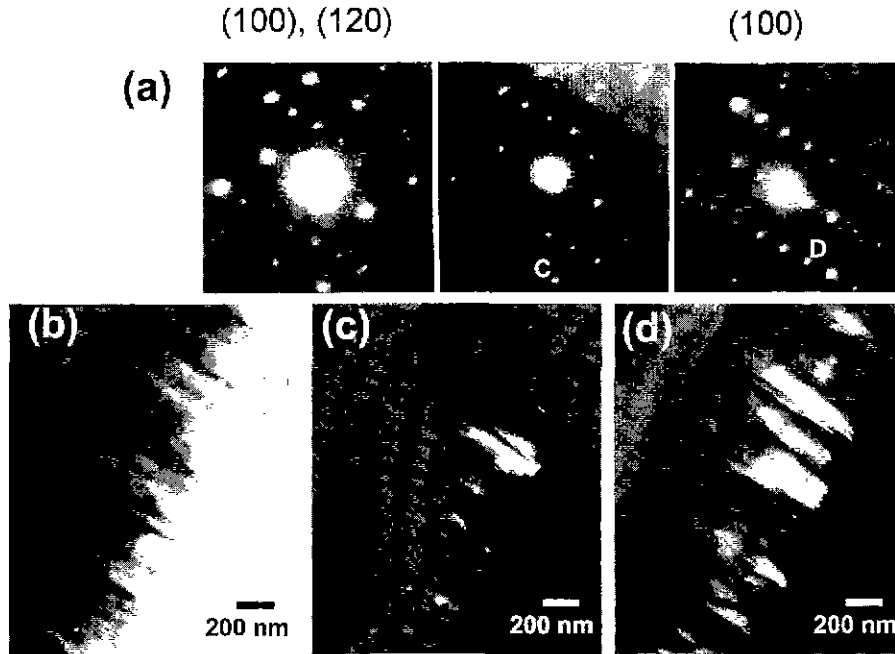


**Fig. 9.** TEM micrographs of an AlN thin film deposited at Ar/N<sub>2</sub>=6/2 mTorr and 180 W: (a) SADPs of the areas along the film near surface, (b) bright field image including the areas of diffraction patterns in (a), (c) dark field of spot C( $g=2\bar{1}2$ ) in (a) and (d) dark field of spot D ( $g=012$ )

substrate floating potential.

TEM analyses were performed to observe growth and crystal structure in finer scale. It was hard to make uniform thinning by ion milling because of higher hardness of AlN film than Si substrate. Therefore, near-interface region (Fig. 8(a)) and near-surface region (Fig. 8(b)) were separately observed. Although thick specimen limited

the observation of detailed grain boundaries, SADPs (selected area diffraction pattern) showed that randomly distributed small grains were included in bottom layer. But after the film was grown to thicker than 4000Å, it was composed of parallel columnar grains and showed better crystalline alignment. In the surface region, there were domains composed of larger grains with low-angle grain boundaries confirmed by dark field images and SADPs, as shown in Fig. 9.

This tendency of structural development from random to texture can be explained by the 'self-texture' proposed by Fujimura *et al.*<sup>25)</sup> They reported that surface energy and formation of tetrahedral bonding units are key parameters for texture formation.

SAW devices were fabricated in order to evaluate AlN thin films. Frequency responses of the devices showed that phase velocity range lied in the range of 4925~4960 m/s with center frequency range of 158~160 MHz. Two examples are shown in Fig. 10. This SAW velocity is lower than theoretical value (Rayleigh wave) of 5607 m/s.<sup>6)</sup> But compared to the reported values<sup>1-3)</sup> in the range of 3500~5700 m/s with Si substrates, the AlN thin films can be used for SAW devices.

#### IV. Conclusion

We deposited highly c-axis aligned AlN thin films on SiO<sub>2</sub>/Si substrates applicable for SAW devices by adjusting the deposition condition. Effects of deposition parameters on the microstructure of the films were also studied. Under the deposition condition of Ar/N<sub>2</sub>=6/2

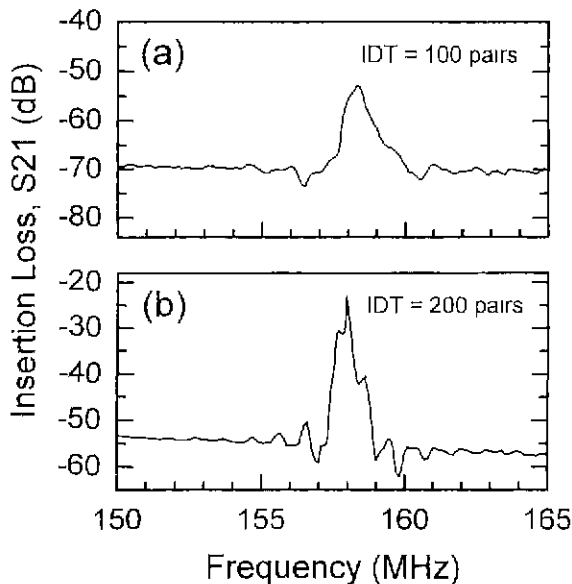


**Fig. 10.** Frequency responses of SAW filters of IDT/AlN/SiO<sub>2</sub>/Si. AlN films were deposited at Ar/N<sub>2</sub>=6/2 mTorr for 240 min, (a) 150 W and (b) 180 W. IDT configuration.  $\lambda=31.2$   $\mu$ m and beam aperture=312  $\mu$ m.

mTorr and 180 W, the film had the best c-axis alignment, which was confirmed by XRD rocking curve (FWHM=2.2°,  $\sigma=0.93^\circ$ ).

Under the low pressure condition (Ar/N<sub>2</sub>=3/2 mTorr), films were peeled off because of stress build-up resulted from atomic peening. For the higher pressure (Ar/N<sub>2</sub>=8/2 mTorr), c-axis alignment was suppressed and the film had columnar structure with loose boundaries.

Cross-sectional TEM analyses showed the development of self-aligned structure after slightly random growth at the initial stage. The columnar grains strongly aligned to the growth direction and had slight alignments to in-plane directions.

SAW device fabricated of these AlN thin films had its phase velocity of about 4950 m/s. Consequently, AlN films on SiO<sub>2</sub>/Si substrates with high c-axis alignment can be used as the materials for SAW devices.

### Acknowledgements

This study was supported by the financial assistance of Ministry of Education Research Fund for Advanced Materials in 1996. The authors would like to thank Dr. H. D. Kwon and S. W. Jang at Oriental Electronics Co. LTD. for their assistance in the characterization of SAW devices.

### References

1. J. K. Liu, K. M. Lakin and K. L. Wang, "Growth Morphology and Surface-acoustic-wave Measurements of AlN films on Sapphire," *J. Appl. Phys.*, **46**[9], 3703-3706 (1975).
2. T. Shiosaki, T. Yamamoto, T. Oda and A. Kawabata, "Low-temperature Growth of Piezoelectric AlN film by rf Reactive Planar Magnetron Sputtering," *Appl. Phys. Lett.* **36**[8], 643-645 (1980).
3. L. G. Pearce, R. L. Gunshor and R. F. Pierret, "Aluminum Nitride on Silicon surface Acoustic wave Devices," *Appl. Phys. Lett.*, **39**[11], 878-879 (1981).
4. K. Tsubouchi and N. Mikoshiba, "Zero-temperature-coefficient SAW Devices on AlN Epitaxial Films," *IEEE Trans. Sonics Ultrason.*, **SU-32**[5], 634-644 (1985).
5. C. Caliendo, G. Saggio, P. Verardi and E. Verona, "Piezoelectric AlN film for SAW Devices Application," *Proc. 1993 IEEE Ultrason. Symp.*, 249-252 (1993).
6. H. Okano, N. Tanaka, Y. Takahashi, T. Tanaka, K. Shibata and S. Nakano, "Preparation of Aluminum Nitride thin Films by Reactive Sputtering and their Application to GHz-band Surface Acoustic wave Devices," *Appl. Phys. Lett.* **64**[2], 166-168 (1994).
7. J. W. Soh, W. J. Lee, J. H. Park and S. W. Lee, "SAW Characteristics of AlN Films Deposited on Various Substrates Using ECR Plasma Enhanced CVD and Reactive RF Sputtering," *Proc. 1996 IEEE Ultrason. Symp.*, 299-302 (1996).
8. Y. J. Yong and J. Y. Lee, "Characteristics of Hydrogenated Aluminum Nitride Films Prepared by Radio Frequency Sputtering and their Application to Surface Acoustic wave Devices," *J. Vac. Sci. Technol. A* **15**[12], 390-393 (1997).
9. W. J. Meng, J. Heremans and Y. T. Cheng, "Epitaxial Growth of Aluminum Nitride on Si(111) by Reactive Sputtering," *Appl. Phys. Lett.* **59**[17], 2097-2099 (1991).
10. K. Tominaga, S. Iwamura, Y. Shuntani and O. Tada, "High-energy Particles in AlN Film Preparation by Reactive Sputtering Technique," *Jpn. J. Appl. Phys.*, **22**[3], 418-422 (1983).
11. M. Akiyama, H. R. Kokabi, K. Nonaka, K. Shobu and T. Watanabe, "Influence of Substrate Temperature on Physical Structure of AlN thin Films Prepared on Polycrystalline MoSi<sub>2</sub> by rf Magnetron Sputtering," *J. Am. Ceram. Soc.*, **78**[12], 3304-3308 (1995).
12. M. H. Francombe and S. V. Krishnaswamy, "Ferroelectric films-growth, Properties and Applications," *Proc. MRS symp.*, **200**, 179-191 (1990).
13. R. B. Stokes and J. D. Crawford, "X-Band thin Film Acoustic Filters on GaAs," *IEEE Trans. on Microwave Theory and Techniques*, **41**[6/7], 1075-1080 (1993).
14. K. M. Lakin, G. R. Kline and K. T. McCarron, "High Q Microwave Acoustic Resonators and Filters," *Proc. 1993 IEEE MTT-S Digest*, 1517-1520 (1993).
15. H. Windischmann, "Intrinsic Stress in AlN Prepared by Dual-ion-beam Sputtering," *Thin Solid Films*, **154**, 159-170 (1987).
16. H. Holleck, "Material Selection for Hard Coatings," *J. Vac. Sci. Technol. A* **4**[6], 2661-2669 (1986).
17. I. Ivanov, L. Hultman, K. Järrendahl, P. M. rtensson, J.-E. Sundgren, B. Hjörvarsson and J. E. Greene, "Growth of Epitaxial AlN (0001) on Si (111) by Reactive Magnetron Sputter Deposition," *J. Appl. Phys.*, **78**[9], 5721-5726 (1995).
18. G. Este, R. Surridge and W. D. Westwood, "Reactively Sputtered AlN Films for GaAs Annealing Caps," *J. Vac. Sci. Technol. A* **4**, 989-992 (1986).
19. G. Este and W. D. Westwood, "Stress Control in Reactively Sputtered AlN and TiN Films," *J. Vac. Sci. Technol. A* **5**[4], 1892-1897 (1987).
20. G. L. Huffman, D. E. Fahline, R. Messier and L. J. Pilione, "Stress Dependence of Reactively Sputtered Aluminum Nitride thin Films on Sputtering Parameters," *J. Vac. Sci. Technol. A* **7**[3], 2252-2255 (1989).
21. S. Onishi, M. Eschwei, S. Bielaczy and W.-C. Wang, "Colorless, Transparent, C-oriented Aluminum Nitride Films Grown at low Temperature by a Modified Sputter Gun," *Appl. Phys. Lett.*, **39**[8] 643-645 (1981).
22. A. Rodriguez-Navarro, W. Ota o-Rivera, J. M. Gar a-Ruiz, R. Messier and L. J. Pilione, "Development of Preferred Orientation in Polycrystalline AlN thin Films Deposited by rf Sputtering System at low Temperature," *J. Mater. Res.*, **12**[7], 1850-1855 (1997).
23. J. A. Thornton, "The Microstructure of Sputter-deposited Coatings," *J. Vac. Sci. Technol. A* **4**[6], 3059-3065 (1986).
24. R. Messier, A. P. Giri and R. A. Roy, "Revised Structure zone Model for thin Film Physical Structure," *J. Vac. Sci. Technol. A* **2**[2], 500-503 (1984).
25. N. Fujimura, T. Nihihara, S. Goto, J. Xu and T. Ito, "Control of Preferred Orientation for ZnO<sub>x</sub> Films: Control of Self-texture," *J. Crystal Growth*, **130**, 269-279 (1993).